www.czasopisma.pan.pl PAN POLSKA AKADEMIA NAUK www.journals.pan.pl

Arch. Min. Sci. **64** (2019), 4, 687-707

Electronic version (in color) of this paper is available: http://mining.archives.pl

DOI 10.24425/ams.2019.129377

RONGBIN HOU**,***, KAI ZHANG*#, JING TAO*

EFFECTS OF INITIAL DAMAGE ON TIME-DEPENDENT BEHAVIOR OF SANDSTONE IN UNIAXIAL COMPRESSIVE CREEP TEST

WPŁYW USZKODZEŃ POCZĄTKOWYCH NA PRZEBIEG CZASOWY ZMIAN ZACHOWANIA PIASKOWCA W TRAKCIE PRÓBY JEDNOOSIOWEGO PEŁZANIA

Time-dependent behavior of rock mass is important for long-term stability analysis in rock engineering. Extensive studies have been carried out on the creep properties and rheological models for variable kinds of rocks, however, the effects of initial damage state on the time-dependent behavior of rock has not yet been taken into consideration. In the present study, the authors proposed a creep test scheme with controlled initial damage to investigate the influence of initial damage on the time-dependent behavior of sandstone. In the test scheme, the initial states of damage were first determined via unloading the specimen from various stresses. Then, the creep test was conducted under different stress levels with specific initial damage. The experimental results show that there is a stress threshold for the initial damage to influence the behavior of the rock in the uniaxial compressive creep tests, which is the stress threshold of dilatancy of rock. When the creep stress is less than the stress threshold, the effect of the initial damage seems to be insignificant. However, if the creep stress is higher than the stress threshold, the initial damage has an important influence on the time-dependent deformation, especially the lateral and volumetric deformation. Moreover, the initial damage also has great influence on the creep failure stress and long-term strength, i.e., higher initial damage leading to lower creep failure stress and long-term strength. The experimental results can provide valuable data for the construction of a creep damage model and long-term stability analysis for rock engineering.

Keywords: multi-loading uniaxial creep test; initial damage; time-dependent behavior; sandstone

Przebieg czasowy zachowania górotworu jest zagadnieniem kluczowym w analizie stabilności systemu w ujęciu długoterminowym. Przeprowadzono szerokie badania modeli reologicznych i właściwości procesów pełzania dla rozmaitych typów skał; jednakże w badaniach nie uwzględniano wpływu uszkodzeń

* CHINA UNIVERSITY OF MINING & TECHNOLOGY, STATE KEY LABORATORY FOR GEOMECHANICS & DEEP UNDERGROUND ENGINEERING, XUZHOU 221116, JIANGSU, CHINA

** CHINA UNIVERSITY OF MINING & TECHNOLOGY,SCHOOL OF MECHANICS & CIVIL ENGINEERING, XUZHOU 221116, JIANGSU, CHINA

*** NORTH CHINA UNIVERSITY OF WATER RESOURCES AND ELECTRIC POWER, SCHOOL OF CIVIL ENGINEERING AND COMMUNICATION, ZHENGZHOU 450045, HENAN, CHINA

Corresponding author: kzhang@cumt.edu.cn

początkowych na zachowanie górotworu i jego przebieg czasowy. W artykule autorzy zaproponowali nowy sposób przeprowadzania próby pełzania, z uwzględnieniem kontrolowanych uszkodzeń początkowych, tak by wpływ obecności uszkodzeń początkowych na przebieg czasowy zmian zachowania piaskowca mógł zostać uwzględniony. W metodzie tej w pierwszej fazie określono zakres początkowych uszkodzeń poprzez odprężenie próbki w celu wyeliminowania rożnego rodzaju naprężeń. Następnie przeprowadzono próbę pełzania w warunkach zmiennych obciążeń przykładanych do próbki o określonym poziomie uszkodzeń początkowych. Wyniki eksperymentu wskazują na istnienie pewnej wartości progowej naprężenia powyżej której obecność uszkodzeń początkowych będzie mieć wpływ na zachowanie próbki skalnej w trakcie próby jednoosiowego pełzania; jest to poziom progowy dla powstawania dylatacji. Gdy naprężenie pełzania ma wartość niższą od wartości progowej, wpływ uszkodzeń początkowych wydaje się nieznaczny. Jednakże, dla naprężeń pełzania powyżej wartości progowej, wpływ uszkodzeń początkowych na przebieg odkształceń jest znaczący, zwłaszcza w odniesieniu do odkształceń poprzecznych i objętościowych. Ponadto, istnienie uszkodzeń początkowych ma także wpływ na poziom naprężeń rozrywających przy próbie pełzania i wytrzymałość próbki w ujęciu długoterminowym. Wykazano, że im większe uszkodzenia początkowe, tym niższa wartość naprężenia zrywającego przy próbie pełzania i niższa wytrzymałość długoterminowa. Wyniki eksperymentu dostarczyć mogą cennych danych niezbędnych do skonstruowania modelu uszkodzeń skał wskutek pełzania oraz do analiz stabilności konstrukcji inżynierskich w ujęciu długoterminowym.

Słowa kluczowe: próba pełzania jednoosiowego przy wielokrotnym obciążeniu, uszkodzenia początkowe, czasowy przebieg zachowań górotworu, piaskowiec

List of Symbols:

D – scalar damage variable
D_{init} – initial state scalar damage variable
ε – axial total strain
ε' – residual strain after unloading
E' – unloading modulus
E – initial Young's modulus
ε_u – crack compaction strain
ε_v – volumetric strain
ε_1 – axial strain
ε_2 – lateral strain

1. Introduction

The creep property of rock mass is important for the long-term stability assessment for rock engineering (Yang et al., 1999; Malan, 1999; Li & Xia, 2000; Kortas, 2013; Kozubal et al., 2016; Zhang et al., 2016). Many researchers have investigated the time-dependent behavior of rock via experiments in the laboratory or field (Gatelier et al., 2002; Yuan et al., 2006; Tsai et al., 2008; Okubo et al., 2010; Zhang et al., 2012; Yang et al., 2014; Kortas, 2016). Based on the experimental results, a number of creep models for the rock mass were proposed (Xu et al., 2006; Weng et al., 2010; Yang & Cheng, 2011; Wang et al., 2013; Ma et al., 2017). Among these creep models, some took damage into consideration, which showed that the time-dependent deformation and damage are coupled with each other (Cao et al., 2016; Ma et al., 2017). However, most of the creep damage models were proposed based on the phenomenology of the experimental results, and few tests were designed to study the coupling characteristic of damage and time-dependent behavior of rock. The present study focuses on the experimental investigation of the effect of the initial damage on the time-dependent behavior of rock.

Excavation is a common activity in rock engineering (e.g. caverns in hydropower station, roadways in underground coal mines). During the excavation, the stress in the surrounding rock will redistribute, and the rock mass may undergo failure and damage. The results of in-situ tests and numerical analysis show that at different depths from the surrounding surface, the rock mass presents different degrees of damage (Wang et al., 2002; Bobet, 2009; Yan et al., 2015; Zhang et al., 2015; Zhang et al., 2018). However, studying the mechanical behavior of the damaged rock mass is critical important for the short-term and long-term stability of the rock engineering. As for the long-term stability assessment of the rock engineering, the time-dependent behavior of rock mass with different degrees of initial damage should be well investigated.

In order to investigate the effects of initial damage on creep characteristic of rock, a creep test scheme with controlled initial damage was proposed. In the test scheme, the initial state of damage was determined via unloading the specimen from various stresses. Then, the uniaxial compressive creep tests were conducted under different stress levels with specific initial damage. Finally, the influence of initial damage on the time-dependent deformation, the creep failure stress and the long-term strength of rock was analyzed.

2. Experimental material and method

2.1. Experiment apparatus

The creep tests were performed on a triaxial testing apparatus, which was designed by the Institute of Rock and Soil Mechanics, Chinese Academy of Sciences (Fig. 1). During the uniaxial compressive creep test, the axial stress is loaded by a high-precision pump, which is automatically controlled by the computer. The axial and radial strains are measured by a pair of LVDTs (Linear

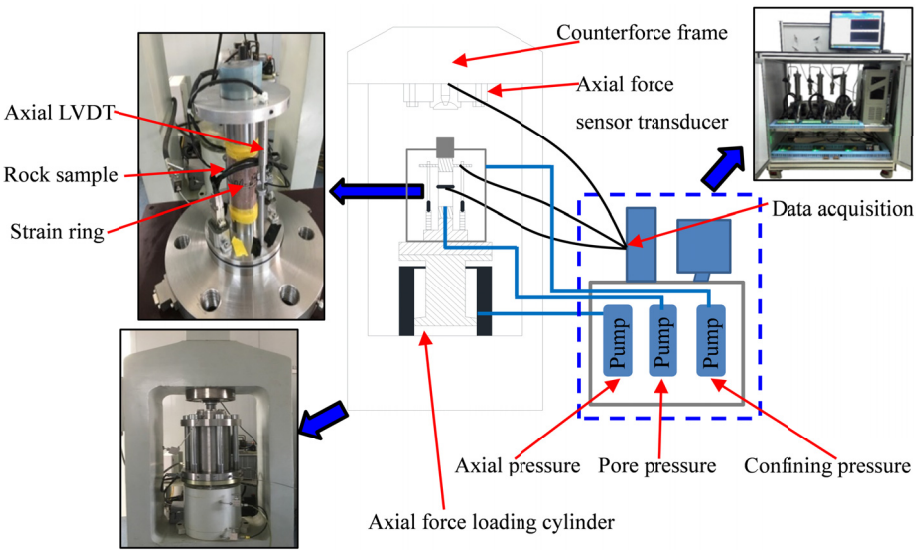

Fig. 1. Illustration of triaxial testing apparatus

Variable Displacement Transducer) and a specifically designed chain collar, respectively. The data of stress and corresponding deformation are recorded by the acquisition system.

2.2. Experimental specimens

The sandstone samples were cored from intact blocks, which are characterized by brown red, coarse grain structure and uniform texture. They were prepared as cylindrical specimens with a diameter 50 mm and a length 100 mm (Fig. 2), in accordance with the experiment specification recommended by the International Society of Rock Mechanics. At room temperature, three specimens were prepared for the uniaxial compressive tests. A typical stress-strain curve of the uniaxial compressive test is shown in Fig. 3. The average values of uniaxial compressive

Fig. 2. Rock specimens of sandstone

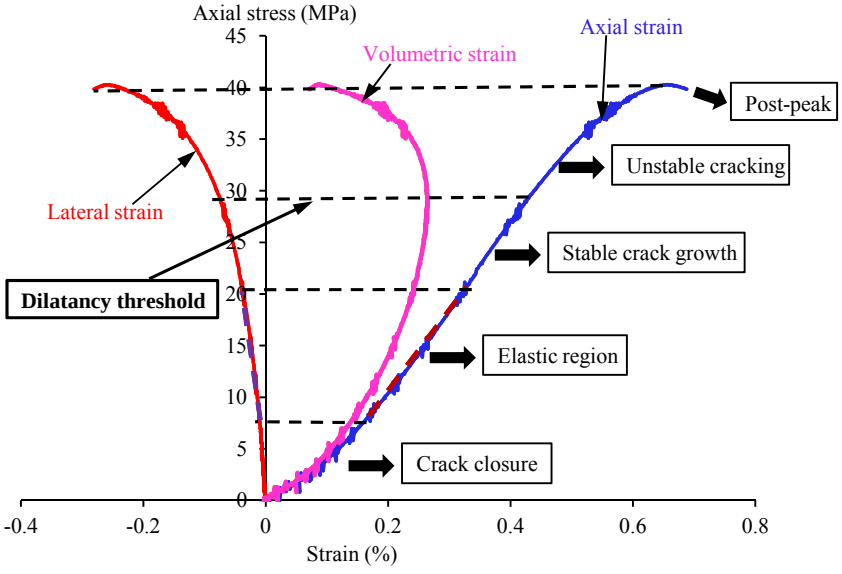

Fig. 3. Stress-strain curve of the uniaxial compressive test of sandstone

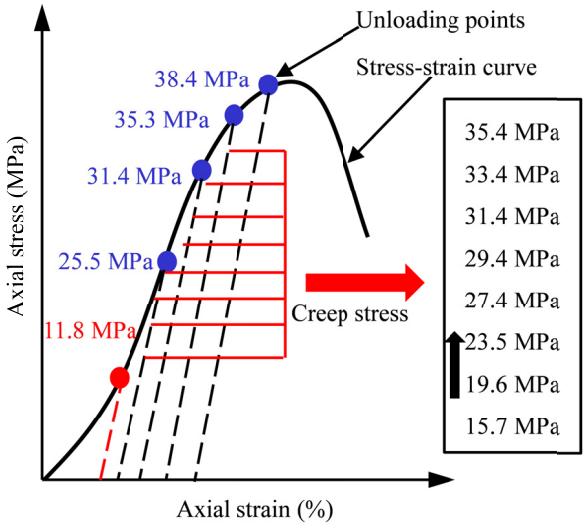

Fig. 4. Schematic diagram of uniaxial compressive creep tests with controlled initial damage

strength, Young's modulus and Poisson's ratio of the sandstone is 39.2 MPa, 9.68 GPa and 0.27, respectively. The standard deviations on uniaxial compressive tests are as: 1.26 MPa for uniaxial compressive strength, 0.15 GPa for Young's modulus and 0.04 for Poisson's ratio.

2.3. Experimental method

It can be seen from Fig. 3 that the deformation characteristics of the rock specimen under uniaxial compression can be divided into five stages (i.e. crack closure, elastic region, stable crack growth, unstable cracking, post-peak). The initial damage state of rock specimens was obtained through the loading-unloading tests. For underground rock engineering, most of the rock mass, which is affected by excavation activities, is in the second, third and fourth stages shown in Fig. 3. Therefore, the unloading stress levels were selected between the crack initiation threshold and the peak stress. The uniaxial compressive creep tests with different initial damage state were designed as follows (Fig. 4):

(i) The axial stress of the specimen is applied to 11.8 MPa (i.e. 30% of the peak strength in the elastic region), and then unloaded completely to obtain the unrecoverable strain caused by crack compaction;
(ii) According to the average uniaxial compressive strength, the specimen is loaded to a specific axial stress level which is beyond the crack initiation threshold, and then unloaded completely to obtain the initial damage of the rock specimen;
(iii) The uniaxial compressive creep test with specific initial damage rock specimen is carried out by multi-stage loading.

During the creep tests, the room temperature should be kept at 20±0.5°C. The stress levels in the multi-stage loading creep tests are set at eight values according to the average peak strength of rock. At each creep stress level, the stress is held constant for 24 h until the specimen fails.

In the present study, creep tests were conducted under four initial damage states of rock. The initial damage condition of the rock specimens was obtained through loading and unloading tests. Four unloading stress levels were selected, which correspond to 65%, 80%, 90% and approximatively 98% of the average uniaxial compressive strength, respectively. The values of the unloading stress and the creep stress are listed in Table 1.

TABLE 1

Unloading stress levels and creep stress levels

Unloading stress (MPa)	Axial creep stress (MPa)							
	1st	2nd	3rd	4th	5th	6th	7th	8th
25.5	15.7	19.6	23.5	27.4	29.4	31.4	33.4	35.4
31.4	15.7	19.6	23.5	27.4	29.4	31.4	33.4	35.4
35.3	15.7	19.6	23.5	27.4	29.4	31.4	33.4	35.4
38.4	15.7	19.6	23.5	27.4	29.4	31.4	33.4	35.4

In the multi-stage loading creep tests, the detailed test procedures are as follows:

(i) Put the sample into the test bench, and make sure the axis of the sample is coincident with the loading centerline of test machine;

(ii) Apply the axial stress with a constant loading rate of the axial displacement consistent with the uniaxial compression test (i.e. 0.07 mm/min) until the pre-determined unloading stress in Table 1, and hold the stress for three minutes. After that, unload the axial stress to 0 MPa with the unloading rate of 0.01 MPa/s;

(iii) Apply axial stress at a constant rate of 0.05 MPa/s to the pre-determined creep stress in Table 1, and record the creep deformation for 24 h;

(iv) Continue the creep test with different creep stresses until the specimen fails.

2.4. Definition of initial damage

The initial damage states in the present study are determined based on the applied axial stress. How to reduce the discontinuity between specimens is the key issue to evaluate the damage state of rock by the loading and unloading tests. The longitudinal wave velocity of the rock specimens was tested, and its average value was 2830 m/s. Then, the specimens with the wave velocity from 2730 to 2930 m/s were selected for the next tests. However, because of the complicated structure of rock material, even if the wave velocity is relatively close, the peak strength and strain of different specimens may vary greatly. To solve this problem, Qiu et al. (2012) presented a method that can reduce the discontinuity between different samples, which can estimate the peak strength of similar rock specimens based on the ratio of the threshold of dilatancy stress to the average peak strength.

For the sandstone used in this study, the ratio of the threshold of dilatancy stress to the average peak strength is approximately 0.77 (Fig. 3). During the experiments, the peak strength of the rock specimen was first estimated using the ratio mentioned above. If the predicted peak strength of a specimen is close to the average peak strength, the subsequent tests will be performed; otherwise, the test on the specimen will be ceased.

When the rock samples are loaded, there may be some cracks initiated inside the samples, which will lead to the damage of the material. There are many ways to define the quantity of

damage. Some methods are based on the plastic deformation and AE events (Chen et al., 2014; Chen et al., 2015), while the others are on account of the deterioration of elastic parameters, e.g. Young's modulus (Xie et al., 1997; Fan & Jin, 2000). Based on the isotropic assumption, Xie et al. (1997) presented an equation to describe the damage of rock material using the variation of strain and Young's modulus as follows:

$$D = 1 - \frac{\varepsilon - \varepsilon'}{\varepsilon}\left(\frac{E'}{E}\right) \tag{1}$$

Where D denotes the damage variable of rock, ε denotes the total axial strain, ε' denotes the residual axial strain after unloading, E' denotes the unloading modulus, E denotes the initial Young's modulus.

In Eq. (1), the residual axial strain after unloading contains both the non-recoverable strain induced by crack compaction and the plastic strain induced by crack propagation. However, the non-recoverable strain induced by crack compaction is always ignored in the constitutive models, as it may be influenced by the sampling process greatly. Therefore, when defining the initial damage variable of rock based on Eq. (1), it should not be considered the crack compaction strain, and the equation for calculating the quantity of initial damage of rock is proposed as follows:

$$D_{init} = 1 - \frac{\varepsilon - \varepsilon'}{\varepsilon - \varepsilon_u}\left(\frac{E'}{E}\right) \tag{2}$$

Where, D_{init} denotes the initial damage variable of rock, ε_u denotes the crack compaction strain.

The method of obtaining the material constants in Eq. (2) is shown in Fig. 5. It can be seen from the figure that crack compaction strain (ε_u) is obtained by the first loading and unloading

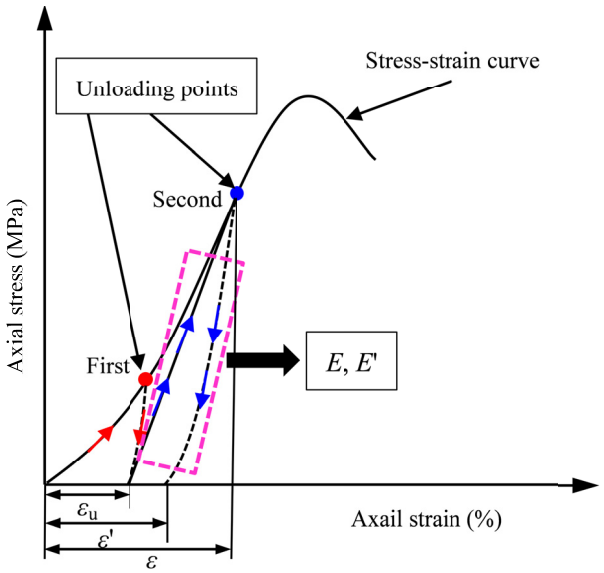

Fig. 5. Method for obtaining the parameters in the equation of the initial damage variable

test, and the other parameters (ε, ε', E, E') are obtained by the second loading and unloading test. Then, substitute the parameters into Eq. (2) to calculate the initial damage variable of rock.

In the present tests, four different initial damage states of samples were prepared. The values of the initial damage variable were calculated by Eq. (2) for each sample, and the results are shown in Table 2. For convenience to the next results analysis, the rock samples that have different initial damage states are denoted D_1, D_2, D_3, and D_4, respectively (shown in Table 2). The relation between the initial damage variable and the unloading stress is shown in Fig. 6. It can be seen that the damage variable increases with the increase of the unloading stress, and the difference of initial damage states between the samples is obvious, which is beneficial to analyze the effects of initial damage on time-dependent behavior.

TABLE 2

Values of the initial damage variable for different specimens

Initial damage state	Unloading stress (MPa)	Value of initial damage
D_1	25.5	0.036
D_2	31.4	0.227
D_3	35.3	0.383
D_4	38.4	0.505

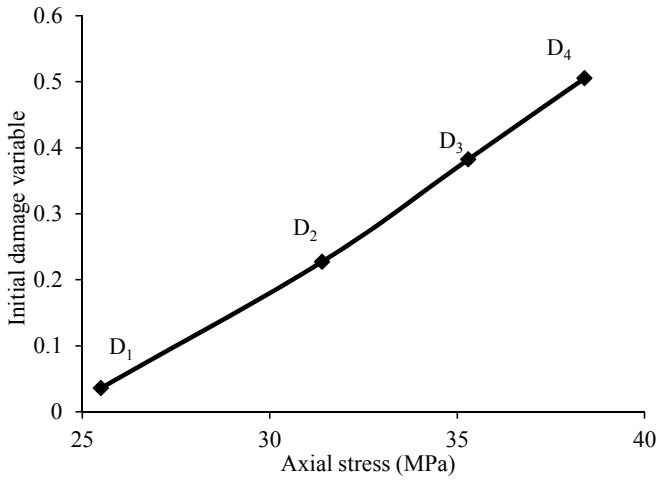

Fig. 6. Relation between initial damage and axial unloading stress

3. Experimental results of time-dependent deformation behavior

In the present research, creep tests under four states of initial damage were conducted. The typical failure morphologies of the specimens are shown in Fig. 7. It can be seen that several tensile cracks are formed in the direction of the axis of the specimens. When the tensile cracks are connected by shear cracks, the specimens fail.

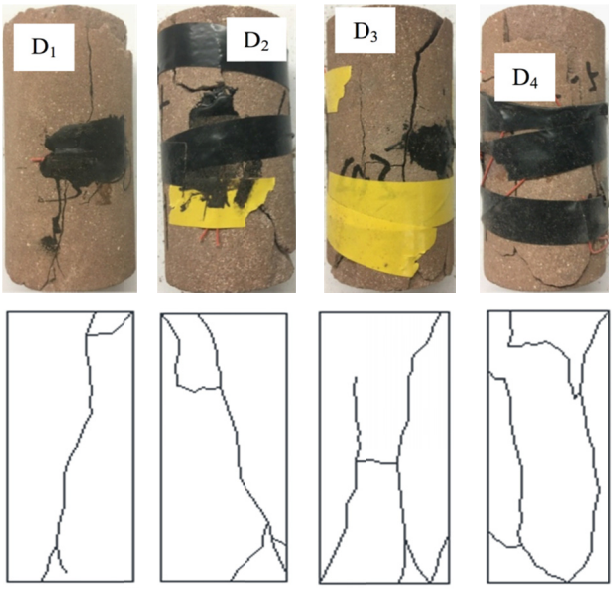

Fig. 7. Typical failure morphologies of the rock specimens

3.1. Axial and lateral strain

The strain curves of uniaxial compressive creep tests with different initial damage are shown in Fig. 8, where the axial compression is positive and the lateral expansion is negative, respectively. It can be seen that the creep curves are smooth without fluctuation, which indicates that the deformation has good continuity with time. For each creep step, the significant instantaneous deformation appears in a sudden manner after the application of load.

At low creep stress levels (i.e. less than 27.4 MPa), the time-dependent deformation (i.e., transient and steady creep deformation) can be observed in the strain curve, and the absolute value of lateral strain is lower than the axial strain. At this stage, the rock is mainly characterized by axial compression and little lateral expansion.

Under the condition of high creep stress levels (i.e. higher than 27.4 MPa), the accelerated creep appears after the transient creep and the steady creep, and the time-dependent failure can be observed in the last loading step. Additionally, with the increase of the creep stress levels, the lateral strain increases more significantly than the axial strain, and gradually becomes to be dominant.

From Fig. 8, it can be seen that the total strain is composed of the instantaneous strain immediately following the applied load and the time-dependent strain (i.e. creep strain) under the constant load. The instantaneous strain is mainly related to the applied stress and loading rate. Fig. 9 shows the relationship between the applied axial stress and the axial instantaneous strain of the specimens with different initial damages. It can be seen that when the loading stress is less than 27.4 MPa, the instantaneous axial strain of specimens increase linearly with the loading stress. However, when the loading stress is higher than 27.4 MPa, the instantaneous axial strain responses nonlinearly, which means that the plastic deformation develops. In addition,

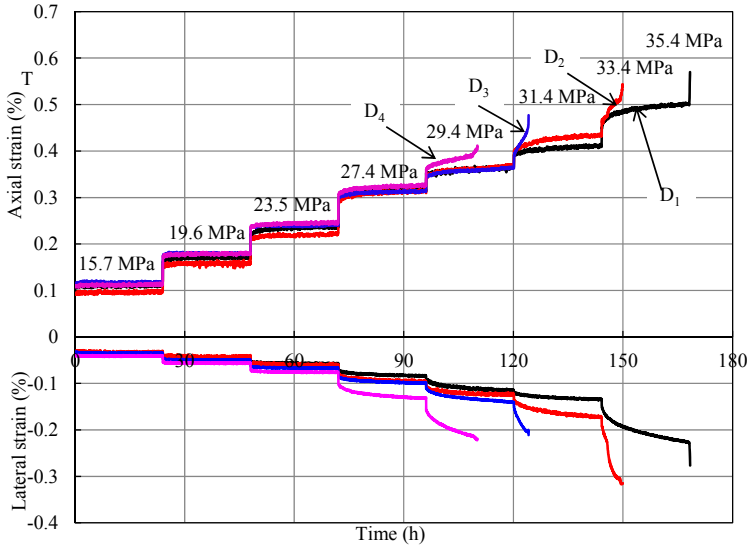

Fig. 8. Axial and lateral strain curves of sandstone with different initial damage under multi-stage axial stress

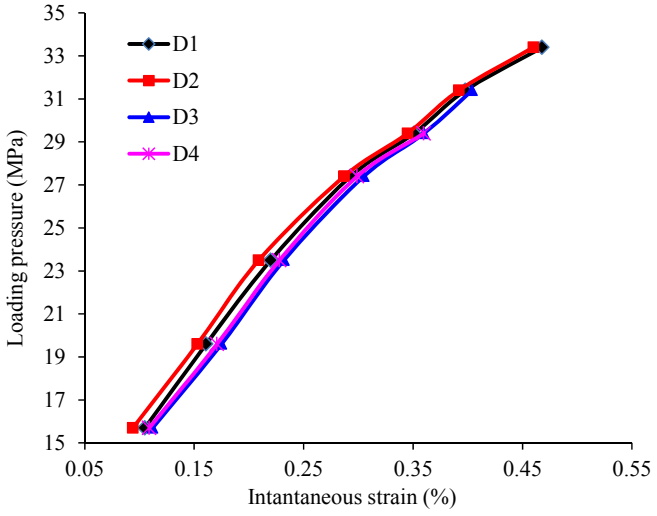

Fig. 9. Relation between loading pressure and axial instantaneous strain of sandstone with different initial damage

it also can be seen from Fig. 9 that the influence of the initial damage on the instantaneous deformation is not remarkable.

The creep strain is obtained by subtracting instantaneous strain from total strain at each creep level. The creep strain under different stress levels is shown in Table 3, and the relation between the creep strain and the creep stress is shown in Fig. 10. It can be seen that the creep

strain increases nonlinearly with the applied creep stress. There is a stress threshold effect on the time-dependent deformation. Below the stress threshold, the initial damage has little influence on the time-dependent deformation. The axial creep strain is greater than the lateral strain. Above the stress threshold, the initial damage has a significant effect on the time-dependent behavior of the rock, and both the axial and lateral creep strain increase quickly with the creep stress. A higher initial damage results in a higher creep strain rates, especially for the lateral creep strain.

TABLE 3

Creep strain under different stress levels of sandstone

Initial damage state	Strain type	Creep strain (10^{-3})						
		1st	2nd	3rd	4th	5th	6th	7th
D_1	axial	0.068	0.129	0.282	0.514	0.716	1.002	1.437
	lateral	–0.029	–0.034	–0.076	–0.217	–0.512	–0.662	–0.864
D_2	axial	0.080	0.150	0.295	0.557	0.756	1.085	1.548
	lateral	–0.037	–0.045	–0.080	–0.222	–0.538	–0.761	–0.966
D_3	axial	0.076	0.130	0.245	0.471	0.695	1.330	/
	lateral	–0.034	–0.040	–0.099	–0.249	–0.722	–1.040	/
D_4	axial	0.092	0.159	0.252	0.494	1.244	/	/
	lateral	–0.040	–0.050	–0.094	–0.395	–1.028	/	/

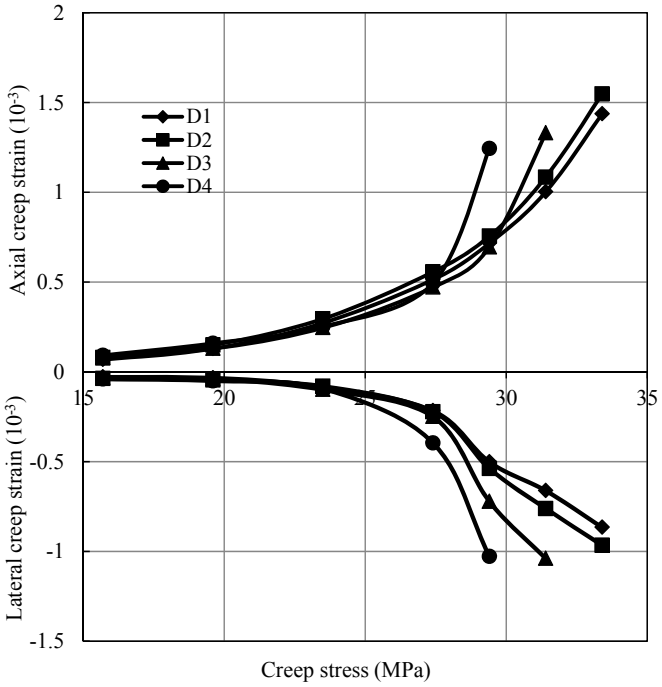

Fig. 10. Relation between creep strain and loading stress of sandstone with different initial damage

3.2. Volumetric strain

Yielding and damage of rock are often accompanied by volumetric dilatancy. According to ISRM suggested methods for determining the creep characteristics of rock (Aydan et al., 2014), a cylindrical sample subjected to axial loading, without a confining stress and under small strains, the volumetric strain (ε_v) is given by Eq. (3). The relationship between calculated volumetric strain and time is shown in Fig. 11.

$$\varepsilon_v = \varepsilon_1 + 2\varepsilon_2 \tag{3}$$

Where, ε_v denotes volumetric strain, ε_1 denotes axial strain, ε_2 denotes lateral strain.

From Fig. 11, it can be seen that the volumetric strain presents two characteristics. First, when the axial stress is less than 27.4 MPa, the volumetric strain increases (compression) during applying the axial stress and varies slightly as the stress is kept constant. In this condition, the volumetric strain is little influenced by the initial damage. Second, when the axial stress increases beyond 27.4 MPa, the volumetric strain varies from compression to dilatancy, as represented by the 'A' region in Fig. 11. During this stage, the initial damage has a remarkable effect on the volumetric strain. The specimens with higher initial damage have larger volumetric strain rate, and are more liable to expand and fail.

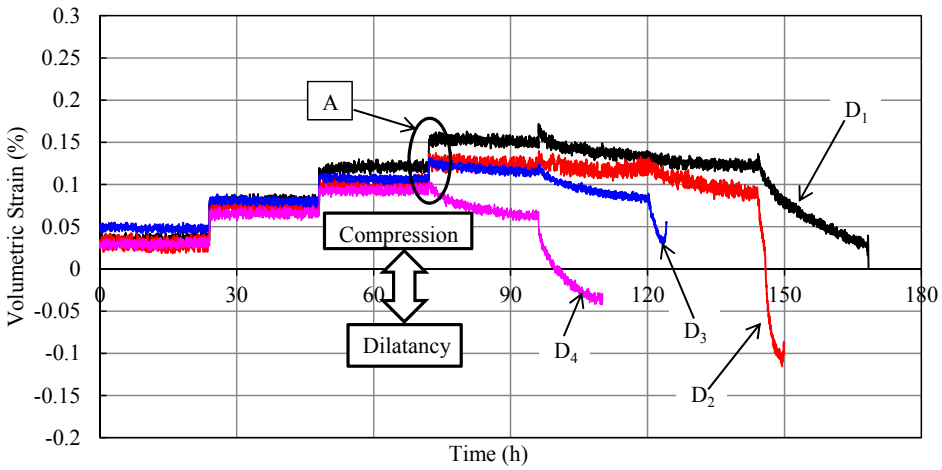

Fig. 11. Volumetric strain curves of sandstone with different initial damage under multi-stage axial stress

In addition, it is interesting to find that the stress threshold of dilatancy seems to be little affected by the initial damage state of the specimens during the creep tests. It is indicated that there is no significant difference in creep characteristics of rocks with different initial damage states at low creep stress levels. However, at the high creep stress levels, the effect of initial damage of rock on the creep characteristics should be deserved attention, especially the creep stress beyond the dilatancy threshold.

4. Creep failure stress with different initial damage

As shown in Fig. 8, in the multi-stage loading creep tests, the time-dependent response of the specimen includes four stages: transient, steady and accelerative creep, and final failure. For the rock specimens with different initial damages, the creep failure stresses are different, and the creep manners before failure also show some distinction. For the specimen with the initial damage of D_1, the creep failure stress is 35.4 MPa. Before the failure of the specimen, the duration of accelerative creep is quite short. For the specimens with the initial damage of D_2 and D_3, the accelerative creep appears shortly following the steady creep stage, and then the rock failed at the axial stress of 33.4 and 31.4 MPa, respectively. For the specimen with the initial damage of D_4, there is a long duration of creep deformation (i.e., the transient, steady and accelerative creep) before the specimen failed, which is approximately 14 hours. From the above observation, it may be concluded that the rock with low damage tends to fail abruptly, while that with high damage may fail gradually with larger deformation.

Fig. 12 shows the relationship between the creep failure stress and the initial damages of rock specimens. It can be seen that the creep failure stress decreases linearly with the increase of the initial damage. From the fitted equation in Fig. 12, when the damage is zero, the creep failure stress is approximately 35.9 MPa, which is approximately 92% of the uniaxial compressive strength (39.2 MPa).

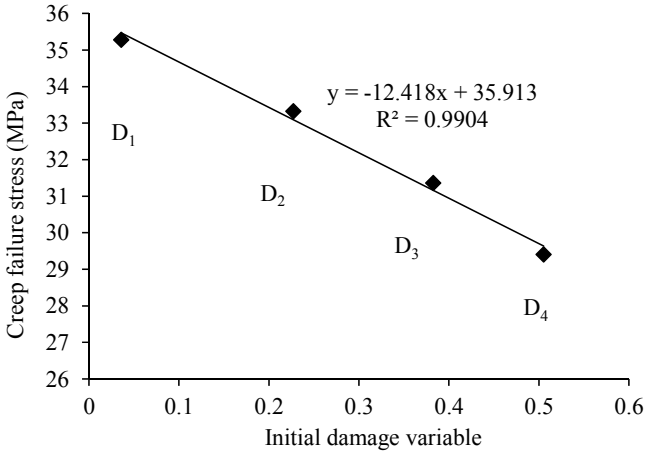

Fig. 12. Relationship between initial damage and creep failure stress

5. Strain rate in creep tests

5.1. Steady creep rate

Following the instantaneous strain, the strain rate decelerates rapidly with time at the transient creep stage until it reaches a nonzero value, which is called steady creep rate. The steady creep rate is the most important index to estimate the long-term deformation of structure. The

axial and lateral steady creep rates of sandstone with different initial damages under different creep stress levels are listed in Table 4. The relation between creep stress and the steady creep strain rate is demonstrated in Fig. 13, except for the last creep stress level. It can be seen that the relationship between the steady creep strain rate and the creep stress should be express by an exponential function. At low creep stress levels, i.e., less than 27.4 MPa, the increase of strain rate is not obvious with the increase of creep stress. But, the steady creep strain rate increases rapidly when the creep stress levels are more than 27.4 MPa.

TABLE 4

Steady creep rate at different creep stress levels

Sample state	Creep stress (MPa)	ASCR (10-4/h)	LSCR (10-4/h)
D_1	15.7	0.006	0.004
	19.6	0.021	0.008
	23.5	0.060	0.018
	27.4	0.092	0.047
	29.4	0.170	0.106
	31.4	0.224	0.153
	33.4	0.319	0.216
D_2	15.7	0.006	0.001
	19.6	0.013	0.003
	23.5	0.062	0.016
	27.4	0.104	0.041
	29.4	0.184	0.109
	31.4	0.237	0.209
	33.4	1.735	0.821
D_3	15.7	0.004	0.001
	19.6	0.016	0.002
	23.5	0.039	0.013
	27.4	0.079	0.051
	29.4	0.147	0.196
	31.4	1.647	1.482
D_4	15.7	0.010	0.004
	19.6	0.019	0.008
	23.5	0.049	0.014
	27.4	0.096	0.109
	29.4	0.611	1.124

Note: ASCR-Axial steady creep rate; LSCR-Lateral steady creep rate

As can be seen from Fig.13, the axial steady creep strain rates of specimens with different initial damage states are approximately consistent at low creep stress level. However, when the creep stress level is more than 27.4 MPa, the regression curves show that the steady creep strain rate is positively correlated with initial damage at same creep stress level. It can be concluded that the influence of initial damage on steady creep strain rate can be neglected at low creep stress levels, but it must be paid attention at the high stress levels.

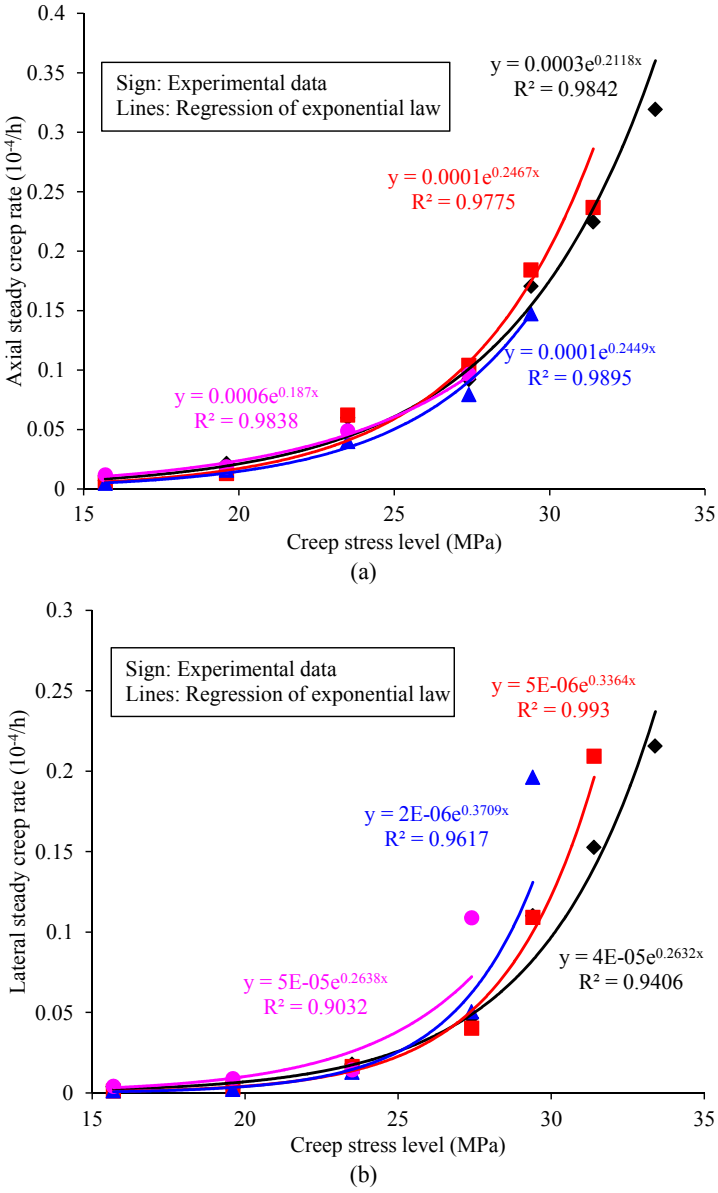

Fig. 13. Correlation between steady creep strain rates and creep stress

5.2. Characteristics of strain rate before creep failure

The rock specimens were terminated by a rupture at the final stress level, i.e. creep failure stress, of the multistage creep tests, except for the specimen with initial damage state D_1, which was terminated in the loading stage. Three distinct creep stages including transient, steady and

accelerative creep could be observed at the last creep stress level before rock specimens fail. For rock specimen, the appearance of accelerative creep stages is related to stress level, time and material properties. In this case, it is impossible to describe the effect of initial damage on the strain rate of rock at the last creep stress level. However, it is helpful to analyze the characteristics of creep damage evolution by studying the variation of the creep strain rate at the last stress level.

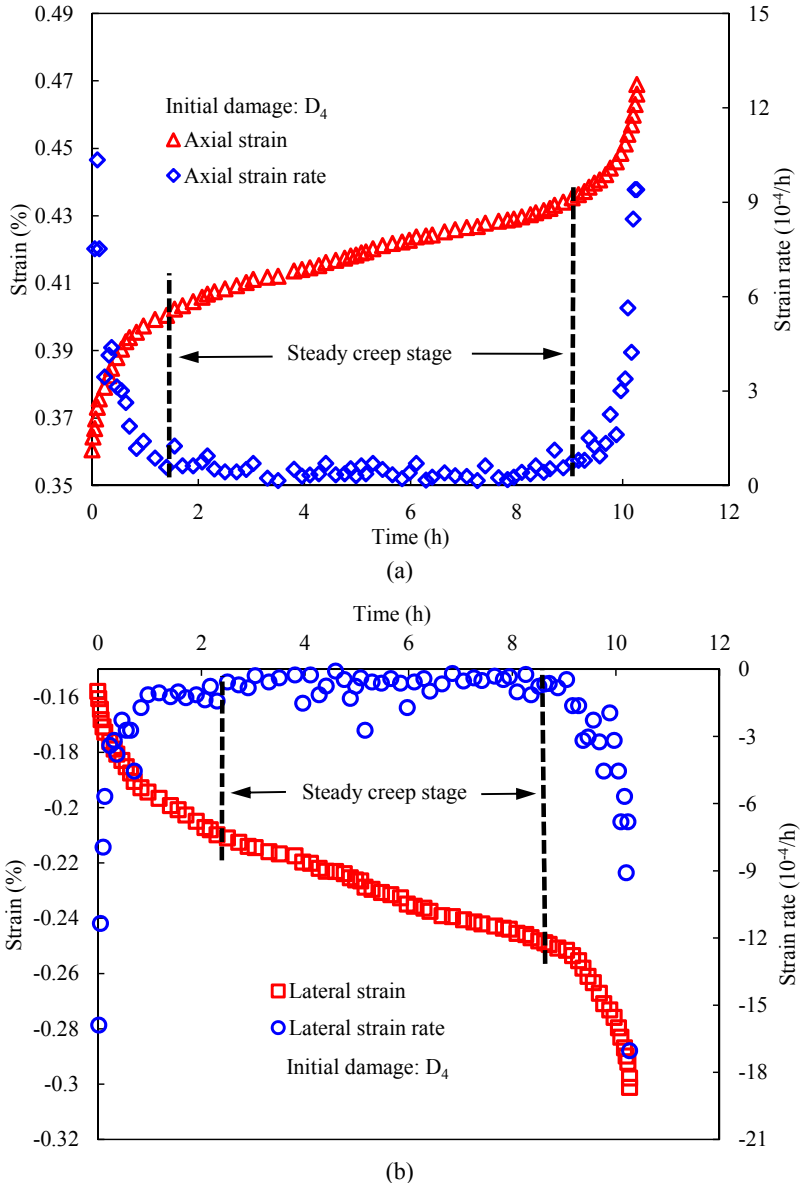

Fig. 14. Creep strain and strain rate characteristics at failure stress of the sample with initial damage state D_4

The time-dependent behaviors of the sample with initial damage state D_4, including the strain and the strain rate at the last creep stress level before failure are plotted in Fig. 14. There is a typical creep curve before creep failure, including transient, steady and accelerative creep (Fig. 14). At the last creep stress level before rock failure, the strain rate first gradually decreases to a constant value in the transient creep stage; then, the strain rate remains constant at the steady creep stage and the deformation increases linearly with time; finally, the deformation increases rapidly with the strain rate increases nonlinearly in the accelerative creep stage until the rock failure (Yang et al., 1999; Li & Xia, 2000). In addition, it can be found from Fig. 14 that the duration of the accelerative creep is much shorter than that in the steady creep stage. Therefore, compared with the steady creep rate, the accelerative creep rate is not suitable for predicting the failure of rock engineering.

As shown in Fig. 14, the creep duration was 10.2 h when the creep stress was 29.4 MPa, and then the creep terminated by a rupture. Compared the axial creep strain rate and the lateral strain rate curves, the steady creep duration in the axial direction was longer than that in the lateral direction, and the accelerative creep occurred earlier in the lateral direction than in the lateral direction. Therefore, it can be inferred that the lateral strain was more sensitive to the load at the creep failure stress levels.

6. Long-term strength of sandstone with different initial damage state

At present, the determination of long-term strength of rock is based on the characteristics of creep curve from the tests. The common analytical method includes drawing isochronous stress-strain curve, finding the stress at volume strain reversal, and identifying the stress causing the steady creep (Chandler, 2013; Liu & Xu, 2015; Lu & Hu, 2017; Wu et al., 2017). From the testing results above, it can be found that significant lateral time-dependent deformation can be observed before the failure of samples. Moreover, Cui (2006) pointed out that considering the lateral creep characteristics of rock to determine the long-term strength is more significance for engineering safety. Therefore, the isochronal stress-strain (lateral strain) curves of sandstone with different initial damage were drawn based on the process introduced by Tan (1982).The results are shown in Fig. 15. Then, the long-term strengths of sandstone with different initial damage are obtained via the isochronal stress-strain curves, and are listed in Table 5.

TABLE 5

Long-term strength of sandstone with different initial damage

Sample state	Values of initial damage	Long-term strength (MPa)
D_1	0.036	32.4
D_2	0.227	30.4
D_3	0.383	28.4
D_4	0.505	25.5

It can be seen from Fig. 15 and Table 4 that the long-term strengths of sandstone with different initial damage are different. The relation between initial damage and long-term strength of

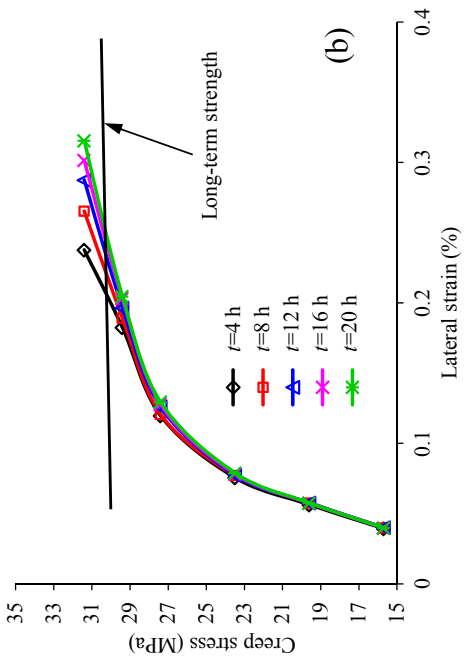

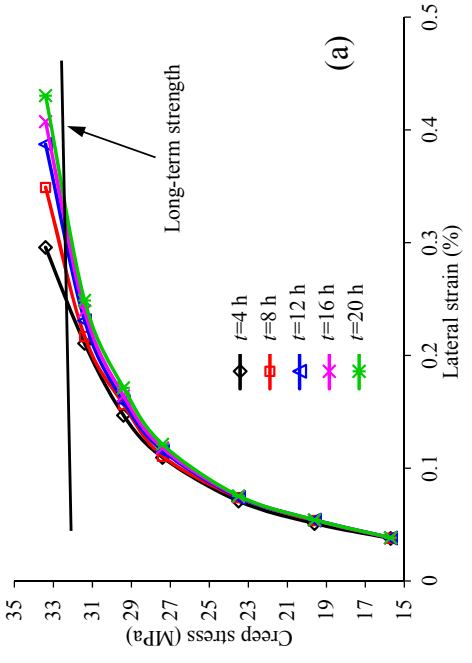

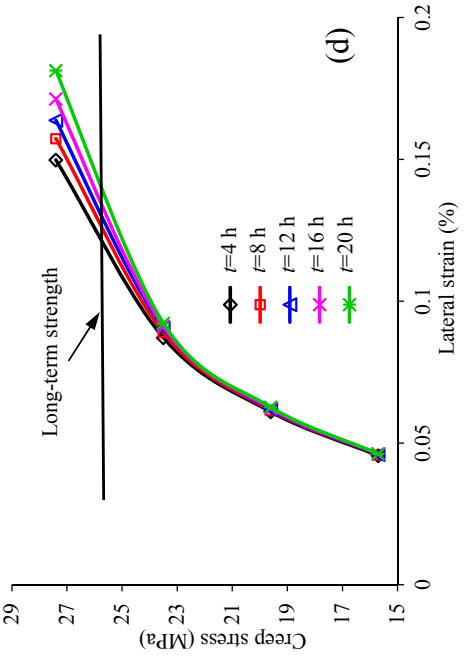

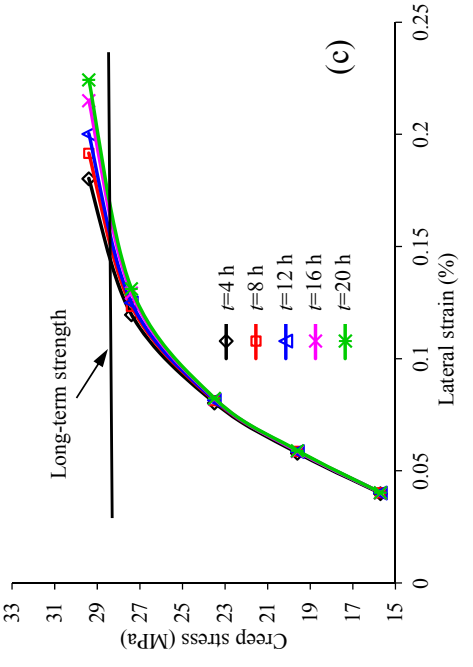

Fig. 15. Isochronous stress-strain of sandstone with different initial damage state: (a), (b), (c), (d) are initial damage state D_1, D_2, D_3, D_4 respectively

sandstone can be described by a linear criterion (Fig. 16). Compared to the compression strength derived from the uniaxial compression test, the long-term compression strength of sandstone with initial damage D_1, D_2, D_3, D_4 decreased by more than 18%, 23%, 28%, 35%, respectively. It means that the larger initial damage of rock is, the more easily the accelerated creep failure occurs for rock engineering. Therefore, considering the influence of initial damage state on the long-term strength is very important for predicting the service life of rock engineering.

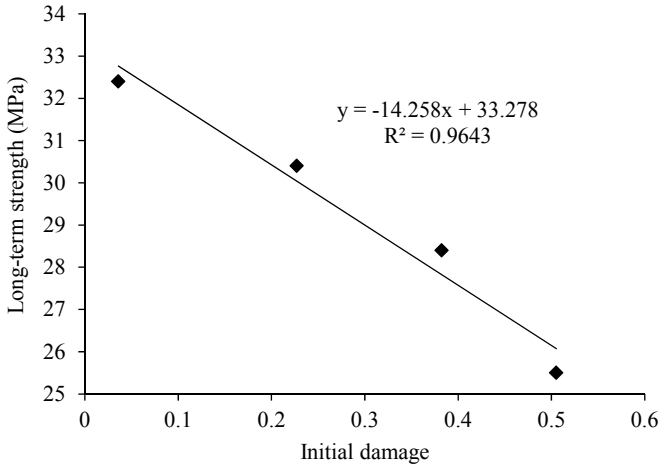

Fig. 16. Relation between long-term strength and initial damage

7. Conclusions

In the present research, on the basis of the experimental results, the influence of initial damage on time-dependent behavior of sandstone is analyzed in detail. The main conclusions are as follows:

(1) The effect of initial damage on time-dependent deformation characteristics is related to the stress of dilatancy threshold. When the applied stress is less than the threshold, the initial damage has little influence on the time-dependent deformation of sandstone. However, if the applied stress is higher than the threshold, the initial damage affects the time dependent deformation significantly, especially the lateral and the volumetric deformation.

(2) The creep failure stress and the long-term strength are strongly affected by the initial damage of rock. That is the rock specimen with larger initial damage has lower creep failure stress. The main feature associated with creep failure presents obvious lateral expansion, high volumetric dilation and steady strain rate. The long-term strength of rock is influenced by the initial damage, and their relationships can be expressed by a linear function.

(3) The initial damage has little influence on the steady creep strain rate at low creep stress levels. However, when the stress levels are higher than the stress of dilatancy threshold, under the same stress conditions the steady creep strain rates are positively correlated

with initial damage states of rock, and especially the initial damage has a significant effect on the lateral strain rate.

(4) Although there are no laws about the influence of initial damage of rock on the time-dependent deformation and strain rate at the creep failure stress level, three distinct creep stages still could be observed in the tests. It is noted that the duration of accelerative creep is much shorter than that of steady creep, and the accelerative creep occurred earlier in the lateral direction than in the lateral direction.

Acknowledgements

This work was supported by the Fundamental Research Funds for the Central Universities (Grant No. Z19012)

References

Bobet A., 2009. *Elastic solution for deep tunnels. Application to excavation damage zone and rockbolt support*. Rock Mechanics and Rock Engineering **42** (2), 147-174.

Cao P., Wen Y.D., Wang Y.X. et al., 2016. *Study on nonlinear damage creep constitutive model for high-stress soft rock*. Environmental Earth Sciences **75**, 900.

Cui X.H., Fu Z.L., 2006. *Experimental study on rheology properties and long-term strength of rocks*. Chinese Journal of Rock Mechanics and Engineering **25** (5), 1021-1024 (in Chinese).

Chandler N.A., 2013. *Quantifying long-term strength and rock damage properties from plots of shear strain versus volume strain*. International Journal of Rock Mechanics and Mining Sciences **59**, 105-110.

Chen L., Liu J.F., Wang C.P. et al., 2014. *Characterization of damage evolution in granite under compressive stress condition and its effect on permeability*. International Journal of Rock Mechanics and Mining Sciences **71**, 340-349.

Chen L., Liu J.F., Wang C.P. et al., 2015. *Damage and plastic deformation modeling of beishan granite under compressive stress conditions*. Rock Mechanics and Rock Engineering **48** (4), 1623-1633.

Fan H.L., Jin F.N., 2000. *Effcetive modulus method in damage mechanics of rock*. Chinese Journal of Rock Mechanics and Engineering **19** (4), 432-435 (in Chinese).

Gatelier N., Pellet F., Loret B., 2002. *Mechanical damage of an anisotropic porous rock in cyclic triaxial tests*. International Journal of Rock Mechanics and Mining Sciences **39** (3), 335-354.

Kortas G., 2013. *Long- and short-term processes indicated by the displacement of the chamber roofs in the monumental wieliczka salt mine*. Archives of Mining Sciences **58** (1), 119-130.

Kortas G., 2016. *Equilizing of the primary stress state in the rock mass, simulated by a model of layer in an elastic-viscous medium*. Archives of Mining Sciences **61** (4), 853-873

Kozubal J., Tomanovic Z., Zivaljevic S., 2016. *The soft rock socketed monopile with creep effects - a reliability approach based on wavelet neural networks*. Archives of Mining Sciences **61** (3), 571-585.

Li Y.S., Xia C.C., 2000. *Time-dependent tests on intact rocks in uniaxial compression*. International Journal of Rock Mechanics and Mining Sciences **37** (3), 467-475.

Liu L., Xu W., 2015. *Experimental researches on long-term strength of granite gneiss*. Advances in Materials Science and Engineering **2**, 1-9.

Lu C., Hu X.L., 2017. *Triaxial rheological property of sandstone under low confining pressure*. Engineering Geology **231**, 45-55.

Malan D.F., 1999. *Time-dependent behaviour of deep level tabular excavations in hard rock*. Rock Mechanics and Rock Engineering **32** (2), 123-155.

Ma L.J., Wang M.Y., Zhang N., et al., 2017. *A variable-parameter creep damage model incorporating the effects of loading frequency for rock salt and its application in a bedded storage cavern*. Rock Mechanics and Rock Engineering **50** (9), 1-15.

Okubo S., Fukui K., Hashiba K., 2010. *Long-term creep of water-saturated tuff under uniaxial compression*. International Journal of Rock Mechanics and Mining Sciences **47** (5), 839-844.

Aydan O., Ito T., Özbay U. et al., 2014. *ISRM Suggested Methods for Determining the Creep Characteristics of Rock*. Rock Mechanics and Rock Engineering **47** (1), 275-290.

Qiu S.L., Feng X.T., Zhang C.Q. et al., 2012. *Experimental research on mechanical properties of deep marble under different initial damage levels and unloading paths*. Chinese Journal of Rock Mechanics and Engineering **31** (8), 1686-1697 (in Chinese).

Tan T., 1982. *The mechanical problems for the long-term stability of underground galleries*. Chinese Journal of Rock Mechanics and Engineering **1** (1), 1-20 (in Chinese).

Tsai L.S., Hsieh Y.M., Weng M.C. et al., 2008 T*ime-dependent deformation behaviors of weak sandstones*. International Journal of Rock Mechanics and Mining Sciences **45** (2), 144-154.

Wu L.Z., Li B., Huang R.Q. et al., 2017. *Experimental study and modeling of shear rheology in sandstone with non-persistent joints*. Engineering Geology **222**, 201-211.

Weng M.C., Tsai L.S., Hsieh Y.M. et al., 2010. *An associated elastic-viscoplastic constitutive model for sandstone involving shear-induced volumetric deformation*. International Journal of Rock Mechanics and Mining Sciences **47** (8), 1263-1273.

Wang W.J., Feng T., Hou C.J. et al., 2002. *Analysis on the relationship between stress distribution on integrated coal beside roadway driving along next goaf and damage of surrounding rocks*. Chinese Journal of Rock Mechanics and Engineering **21** (11), 290-593 (in Chinese).

Wang R.B., Xu W.Y., Wang W. et al., 2013. *A nonlinear creep damage model for brittle rocks based on time-dependent damage*. European Journal of Environmental and Civil Engineering **17** (s1), 111-125.

Xu W.Y., Yang S.Q., Chu W.J., 2006. *Nonlinear viscoelasto-plastic rheological model (hohai model) of rock and its engineering application*. Chinese Journal of Rock Mechanics and Engineering **25** (3), 433-447 (in Chinese).

Xie H.P., Ju Y., Dong Y.L., 1997. *Discussion about "elastic modulus method" in the classic definition of damage*. Mechanics Practice **19** (2), 1-5 (in Chinese).

Yang C.H., Daemen J.J.K., Yin J.H., 1999. *Experimental investigation of creep behavior of salt rock*. International Journal of Rock Mechanics and Mining Sciences **36** (2), 233-242.

Yuan H.P., Cao P., Wan W. et al., 2006. *Study on creep rules of soft and intricate ore-rock under step load and unload*. Chinese Journal of Rock Mechanics and Engineering **25** (8), 1575-1581 (in Chinese).

Yang W.D., Zhang Q.Y., Li S.C. et al., 2014. *Time-dependent behavior of diabase and a nonlinear creep model*. Rock Mechanics and Rock Engineering **47** (4), 1211-1224.

Yang S.Q., Cheng L., 2011. *Non-stationary and nonlinear visco-elastic shear creep model for shale*. International Journal of Rock Mechanics and Mining Sciences **48** (6), 1011-1020.

Yan P., Lu W.B., Chen M. et al., 2015. *Contributions of in-situ stress transient redistribution to blasting excavation damage zone of deep tunnels*. Rock Mechanics and Rock Engineering **48** (2), 715-726.

Zhang Y., Shao J.F., Xu W.Y. et al., 2016. *Time-dependent behavior of cataclastic rocks in a multi-loading triaxial creep test*. Rock Mechanics and Rock Engineering **49** (1), 1-11.

Zhang Z.L., Xu W.Y., Wang W. et al., 2012. *Triaxial creep tests of rock from the compressive zone of dam foundation in xiangjiaba hydropower station*. International Journal of Rock Mechanics and Mining Sciences **50** (35), 133-139.

Zhang K., Zhang G.M., Hou R.B. et al., 2015. *Stress evolution in roadway rock bolts during mining in a fully mechanized longwall face and an evaluation of rock bolt support design*. Rock Mechanics and Rock Engineering **48** (1), 333-344.

Zhang Q., Zhang C.H., Jiang B.S. et al., 2018. *Elastoplastic coupling solution of circular openings in strain-softening rock mass considering pressure-dependent effect*. International Journal of Geomechanics **18** (1), 04017132.